



## Structural characterization of polysaccharides after fermentation from *Ganoderma lucidum* and its antioxidant activity in HepG2 cells induced by H<sub>2</sub>O<sub>2</sub>

Yang Zhao<sup>a,b</sup>, Qinyang Li<sup>c</sup>, Minghui Wang<sup>a</sup>, Yuhua Wang<sup>a</sup>, Chunhong Piao<sup>a</sup>, Hansong Yu<sup>a</sup>, Junmei Liu<sup>a,\*</sup>, Zhuowei Li<sup>d,\*</sup>

<sup>a</sup> College of Food Science and Engineering, Jilin Agricultural University, Changchun 130118, China

<sup>b</sup> Department of Environmental Science & Engineering, Fudan University, Shanghai 200438, China

<sup>c</sup> School of Life Science, Jilin University, Changchun 130012, China

<sup>d</sup> Changchun Vocational Institute of Technology, Changchun 130033, China

### ARTICLE INFO

#### Keywords:

*Ganoderma lucidum*  
Polysaccharide  
Structure  
Antioxidant activity

### ABSTRACT

In this study, *Lactiplantibacillus plantarum* ATCC14917 was used to ferment *Ganoderma lucidum* spore powder. Two polysaccharides were purified from unfermented (GLP) and fermented (FGLP) *Ganoderma lucidum* spore powder. The chemical structure and antioxidant activity of the polysaccharides were studied. Finally, the effect of GLP and FGLP on the oxidative stress regulation pathway in HepG2 cells was explored. The results showed that the main structural characteristics of *Ganoderma lucidum* polysaccharides remained unchanged during the fermentation. However, the average molecular weight ( $M_w$ ) of *Ganoderma lucidum* polysaccharides decreased from  $1.12 \times 10^5$  Da to  $0.89 \times 10^5$  Da. Besides this, the contents of mannose, galactose, and glucuronic acid increased, while the contents of xylose and glucose were decreased. In addition, the content of uronic acid was raised, and the apparent structure was changed from smooth and hard to porous and loose. In antioxidant studies, intracellular ROS and MDA contents in the oxidative stress model were decreased, and T-AOC content was increased under GLP and FGLP intervention. In the investigation of the regulation pathway, Nrf-1 gene expression was up-regulated, and Keap1 gene expression was down-regulated under GLP and FGLP intervention. The antioxidant genes NQO1 and NO-1 expressions were increased to activate the activities of antioxidant enzymes CAT, SOD and GSH-PA to resist oxidative stress. Compared with GLP, FGLP has a stronger regulatory role in this pathway, thus showing more potent antioxidant activity. This experiment is beneficial to the further utilization of *Ganoderma lucidum* spore powder.

### Introduction

To face the improvement of health concepts and requirements in contemporary society, people are searching for materials to regulate oxidative stress in the body (Veljović et al., 2017). *Ganoderma lucidum* Spore powder, a high-value healthcare food, has attracted public attention because of its remarkable antioxidant ability (Cör et al., 2018). *Ganoderma lucidum* polysaccharide (GLP) is the most studied substance in *Ganoderma lucidum* due to its inestimable nutritional value (Garuba et al., 2020). GLP has immunomodulatory (Shi et al., 2013), hypoglycemic (Kan et al., 2015), anti-ulcer (Li et al., 2007), antioxidant activity (Pan et al., 2013), anti-aging (Xu et al., 2019), anti-tumor and other

crucial biological functions (Tan et al., 2018; Zhao et al., 2010). Antioxidant activity of GLP from *Ganoderma lucidum* has become a hot topic, in which Li et al. (Li et al., 2020) have studied the effect of GLP on oxidative stress injury in mouse myoblasts induced by H<sub>2</sub>O<sub>2</sub>. They found that reactive oxygen species (ROS) in cells can be decreased by adding 1 mM of H<sub>2</sub>O<sub>2</sub> into myoblast cells, which would increase the cell survival rate up to 81.70%. Meanwhile, this study has demonstrated that GLP has antioxidant activity.

However, GLP has a considerable molecular weight and a complex structure, making it difficult to absorb efficiently by the human body (Liu et al., 2021). The function of polysaccharides is closely associated with their structures. The structure of polysaccharides can be modified

\* Corresponding authors.

E-mail addresses: [liujunmei@jlau.edu.cn](mailto:liujunmei@jlau.edu.cn) (J. Liu), [784140378@qq.com](mailto:784140378@qq.com) (Z. Li).

<https://doi.org/10.1016/j.fochx.2023.100682>

Received 25 September 2022; Received in revised form 3 March 2023; Accepted 13 April 2023

Available online 23 April 2023

2590-1575/© 2023 The Author(s). Published by Elsevier Ltd. This is an open access article under the CC BY-NC-ND license (<http://creativecommons.org/licenses/by-nc-nd/4.0/>).

through physical and chemical methods. However, these methods have complex operations and high energy consumption. Biological methods (fermentation) can be used to efficiently modify polysaccharides to improve their biological activity (Nie et al., 2019; Sun et al., 2016). For example, *Bacillus* sp. DU-106 fermentation can alter the molecular weight and monosaccharide composition of *Dendrobium officinale* polysaccharide and improve its immune activity (Tian et al., 2019). At present, food production by probiotic fermentation has become a hot topic.

*Lactiplantibacillus plantarum* is a common material for probiotic fermentation. For example, *Lactiplantibacillus plantarum* NCU116 fermentation can alter physicochemical characterization, monosaccharide composition, molecular weight (*M<sub>w</sub>*), and viscosity of *Asparagus officinalis* polysaccharides, leading to their superior antioxidant and immunomodulatory activity (Zhang et al., 2018). The modification of polysaccharides by *Lactiplantibacillus plantarum* has broad application prospects. Currently, abundant investigations focus on natural polysaccharides in *Ganoderma lucidum* spore powder. Nevertheless, there are few reports on *Ganoderma lucidum* spore powder fermentation. Herein we have utilized *Lactiplantibacillus plantarum* ATCC14917 for the fermentation of *Ganoderma lucidum* spore powder. *Lactiplantibacillus plantarum* ATCC14917 is a probiotic with a stable reproductive ability and stable metabolic performance (Li et al., 2018). After fermentation, the fermentation alteration of the structure and antioxidant activity of polysaccharides in *Ganoderma lucidum* spore powder was investigated. Finally, the effect of GLP and FGLP on the oxidative stress regulation pathway in HepG2 cells was explored. The innovation of our study lies in the purpose of improving the value of *Ganoderma lucidum* by using probiotics to ferment *Ganoderma lucidum* spores powder, and comprehensively evaluating the structure and antioxidant activity of *Ganoderma lucidum* polysaccharides in order to explore the mechanism of its antioxidant activity after fermentation. Our investigation may provide a research basis for improving the antioxidant activity of polysaccharides in *Ganoderma lucidum* spore powder fermented by *Lactiplantibacillus plantarum* ATCC14917 and show scientific support for the development of *Ganoderma lucidum* spore powder.

## Materials and methods

### Materials

*Ganoderma lucidum* spore powder is obtained from Changbai Mountain, *Lactiplantibacillus plantarum* (ATCC14917), and HepG2 cells were obtained from the Center for excellence in molecular cell science, Chinese Academy of Sciences, China. *N*-butanol, chloroform, trifluoroacetic acid, pyridine, and silylation reagent were purchased from Sinopharm Chemical Reagent Co., Ltd (Beijing, China), before use without further treatment and purification. Mannose, Ribose, Rhamnose, and other standard monosaccharides, T-2000, T-500, T-70, and other Dextran standards, D<sub>2</sub>O, Fetal bovine serum, DMEM (high glucose) medium, trypsin, MTT, DMSO were purchased from Sigma-Aldrich (USA). Reactive oxygen species (ROS) assay kit and Trace malondialdehyde (MDA) assay kit were purchased from Nanjing Jiancheng Biological Engineering Research Institute Co. LTD. All the other reagents were used analytic purity and purchased from Sinopharm Chemical Reagent Co., Ltd (Beijing, China).

### Fermentation and extraction of polysaccharides from *Ganoderma lucidum* spore powder

#### Fermentation

*Lactiplantibacillus plantarum* ATCC14917 was used to ferment *Ganoderma lucidum* spore powder. 2% (w/w) *Ganoderma lucidum* spore powder was added to MRS Broth medium. *Lactiplantibacillus plantarum* ATCC14917 (10<sup>6</sup> CFU/mL) was added to MRS Broth medium and cultured at 37 °C, with stirring of 90 r/min for 24 h. After fermentation, the supernatant of the fermentation broth was collected.

#### Extraction

Polysaccharides from *Ganoderma lucidum* spore powder were extracted by ultrasonic-assisted extraction. 2.0 g of *Ganoderma lucidum* spore powder was added to 114 mL of H<sub>2</sub>O and extracted in a water bath at 80 °C for 5 h. The solution was centrifuged at 9000 r/min for 20 min to remove the insoluble substance. A rotary evaporator was then used to condense solutions to 1/5 of their original volume. Afterwards, proteins in polysaccharides were eliminated by the Sevag method (Li et al., 2017): one-third volume of the volume of the Sevag reagent (chloroform: *n*-butanol = 4:1, v/v) was added to the solution. The solution was then centrifuged at 1000 rpm for 5 min to remove the oil phase containing protein in the upper layer. This process was repeated several times until there was no white precipitation at the boundary of the reagent layer after centrifugation. The solution was then dialyzed by a dialysis bag with 3000 Da. Ethyl alcohol (4-fold amount) was added to the above solution and stored at 4 °C for 24 h. The polysaccharide precipitates were obtained by centrifugation (9000 r/min, 10 min) and freeze-dehydrated. Finally, crude polysaccharides were obtained and stored at -4 °C.

#### Determination of monosaccharide composition

To clarify the monosaccharide composition of GLP and FGLP, gas chromatography (GC) was performed (Li et al., 2018). First of all, 4.0 M trifluoroacetic acid (TFA, 1 mL) was added to 10 mg of GLP and FGLP samples to hydrolyze at 110 °C for 3 h. After drying, 1 mL of pyridine was added to the hydrolyzed polysaccharide, and then 1 mL of silylation reagent (N, O-bis(trimethylsilyl) trifluoroacetamide (BSTFA): trimethylchlorosilane (TMCS) = 99:1, v/v) was quickly added. The above solution was reacted in a drying oven at 70 °C for 30 min. The temperature of the mixed solution was lowered to room temperature, and the supernatant was taken for GC determination. The monosaccharide standards including rhamnose, arabinose, fucose, xylose, mannose, glucose and galactose were silylated by the same protocol.

Gas chromatographic conditions: A high-performance capillary column, DB-17 (30 mL × 0.25 mm ID, 0.25 μm film thickness, Agilent), was used. Inlet temperature was 280 °C, and FID detector temperature was 300 °C. The carrier gas was nitrogen, and the column pressure was 73.0 kPa. The column flow was 1 mL/min, and the split ratio was 10:1. The temperature was set as 50 °C for 3 min. Then it was increased to 280 °C at 10 °C/min and finally kept 280 °C for 5 min. The injection volume was 1 μL.

#### Determination of molecular weight

High-performance gel permeation chromatography (HPGPC) was used to determine the molecular weight of samples (Wang et al., 2013). The mobile phase (2.5 mg/mL) was used to dilute the sample. 0.45 μm microfiltration membrane was used to remove insoluble impurities. The above solution was then taken for HPGPC determination. The same method was used to determine the Dextran standards of different concentrated molecular weights (5, 25, 50, 80, 150 kDa) and draw the calibration curve. The molecular weight of the samples was calculated by comparing them with Dextran standards.

Chromatographic conditions: TSK Gel 3000SWXL column (7.8 mm × 300 mm) was equipped, and the column temperature was set as 35 °C. The mobile phase was 0.025 M of NaH<sub>2</sub>PO<sub>4</sub>, 0.025 M of Na<sub>2</sub>HPO<sub>4</sub> (pH = 6.7), and 0.05 M of NaN<sub>3</sub>. The flow rate was 0.8 mL/min. The detector was a differential refraction detector (RID) with a constant temperature of 35 °C.

#### FTIR determination

Fourier transform infrared spectra of GLP and FGLP were determined<sup>22</sup>. The wavelength range is 4000–400 cm<sup>-1</sup>.

### NMR spectroscopy

GLP and FGLP (about 30 mg) were dissolved in 0.55 mL D<sub>2</sub>O, respectively, and placed in NMR tubes. Then <sup>13</sup>C NMR and <sup>1</sup>H NMR spectra were measured were recorded (at 60 °C) on JNM-ECZR NMR spectrometer (JEOL, Japan) at 600 and 150 MHz, respectively.

### SEM determination

After the samples were completely dried, the sample surfaces were sputter-coated with gold, and the surface of the samples was scanned by Gemini 360 scanning electron microscope (Zeiss, German). The magnification of the images was 2000 and 5000 times, respectively.

### Cell culture and grouping

HepG2 cells were cultured by referring to HAO's method (Hao, 2018; Chiroma et al., 2020): The medium consists of 10% fetal bovine serum (FBS), 1% penicillin–streptomycin, and 89% DMEM (high glucose). The above cells were incubated under saturated humidity with 5% CO<sub>2</sub> and 95% air. The temperature was set as 37°C.

To determine the effects of different concentrations of GLP and FGLP on cell viability, 100 µL of HepG2 cells were cultured for 24 h, and the waste liquid was discarded. GLP and FGLP with concentrations of 0, 10, 50, 100, 200, 300, 400 and 500 µg/mL were added to the medium, respectively. After culturing for 24 h, the supernatant was discarded. The cell survival rate of each group was measured by the MTT method (Zhu et al., 2017): After discarding the culture medium, 100 µL of MTT (5 mg/mL) was used to treat cells for 4 h without light. After throwing away the supernatant, 150 µL of DMSO was used to make precipitates wholly dissolved. A microplate reader was used to record the absorbance value at 490 nm. Each group was set up with six parallel tests. Cell survival rate was calculated, Eq. (1):

$$R(\%) = (f/f_0) \times 100 \quad (1)$$

Where *R* is cell survival rate, *f* is the absorbance value of the control group, and *f*<sub>0</sub> is the absorbance value of the experimental group.

The optimal concentration of H<sub>2</sub>O<sub>2</sub>, which was used to construct the oxidative stress model, was investigated by the above method, and six parallel tests were also set for each group.

The cell cultures were grouped, and the indexes were determined based on the above analysis.

### Intracellular ROS content analysis

HepG2 cells were treated according to the grouping results. After discarding the culture medium, DCFH-DA (10 µM) was added to treat cells without light at 37 °C for 30 min. After throwing away the supernatant, PBS was used to clean the cells 2 times. After digesting by trypsin, the supernatant was thrown away. The cells were re-suspended by PBS and transferred to a 96-well plate blackboard. A fluorescence microplate reader was used to read the ROS relative intensity of cells. The excitation wavelength was 502 nm, and the emission wavelength was 530 nm.

### Intracellular MDA and T-AOC content analysis

HepG2 cells were treated according to the grouping results. After discarding the culture medium, cells were suspended again using 100 µL PBS. The cells were broken by ultrasound at a power of 300 W. The protein concentration of cells was detected using a BCA kit, while the MDA and the T-AOC content of each group were detected using an MDA kit and T-AOC kit, respectively.

**Table 1**  
The primer of different genes.

Gene name	Name	sequence
Keap1	F	5'-GGCCCTCTCTAGTTCAG-3'
	R	5'-CAGCATAGATACAGTTGTGCAG-3'
Nrf2	F	5'-GCCTGTAGCCGATTACCGAGTG-3'
	R	5'-CATGATGAGCTGTGGACCGCTGTG-3'
HO-1	F	5'-CCTCCCTGTACCACATCTATGT-3'
	R	5'-GCTCTTCTGGGAAGTAGACAG-3'
NQO1	F	5'-CCACCTCTGAGTTCAAGCGATTG-3'
	R	5'-GAGTTCAAGACCAGCCTGACCAAC-3'

**Table 2**  
qRT-PCR reaction system.

Reagent	Amount (µL)
TB Green Premix Ex Taq II (Tli RNaseH Plus) (2 × )	12.5
PCR Forward Primer (10 µM)	1.0
PCR Reverse Primer (10 µM)	1.0
DNA template (<100 ng)	2.0
H <sub>2</sub> O	8.5
Total	25.0

### Intracellular CAT, SOD, and GSH-Px content analysis

HepG2 cells were treated according to the grouping results. After discarding the culture medium, cells were suspended again using 100 µL PBS. The cells were broken by ultrasound at a power of 300 W. The protein concentration of cells was detected using a BCA kit, while the CAT, SOD, and the GSH-Px content of each group was detected using a CAT kit, SOD kit and GSH-Px kit, respectively.

### Gene expression analysis

RNA extraction from HepG2 cells: HepG2 cells were treated according to the grouping results. After discarding the culture medium, 1 mL of Trizol was added to fully lysed the cells. Then, 200 µL of precooled chloroform was mixed with the above solutions and centrifuged at 12000 rpm for 15 min. The upper colourless water was transferred to a new centrifuge tube. An equal volume of precooled isopropanol was added to the new centrifuge tube and centrifuged at 12000 rpm for 5 min to discard the supernatant. The precipitation was dried for 2–5 min, 10–20 µL of DEPC H<sub>2</sub>O was added to dissolve the precipitation.

cDNA reverse transcription: The DNA in the above solutions was removed, and then cDNA was synthesized by reverse transcription. The above operation was performed according to the instructions of the reverse transcription kit (PrimeScript™ RT Reagent Kit with gDNA Eraser).

Primer design: Published Human gene sequence was found in NCBI databases. qRT-PCR primers were designed using the primer design program provided by Sangong Bioengineering (Shanghai) Co., LTD. The primers were synthesized by Kumei Biotechnology (Changchun) Co., LTD. The primers are shown in Table 1.

qRT-PCR: Sample loading solution was prepared according to Table 2, and then the obtained cDNA was amplified by qRT-PCR. The conditions are as follows: predenaturation at 95 °C for 30 s, denaturation at 95 °C for 10 s, annealing at 57 °C for 30 s, and extension at 72 °C for 30 s. The total number of cycles was set as 40 cycles. The melting curve was set automatically according to the instrument program. At the end of amplification, Ct values were recorded, and then 2<sup>-ΔΔCt</sup> method (Livak and Schmittgen, 2001) was used to calculate mRNA relative expression levels.

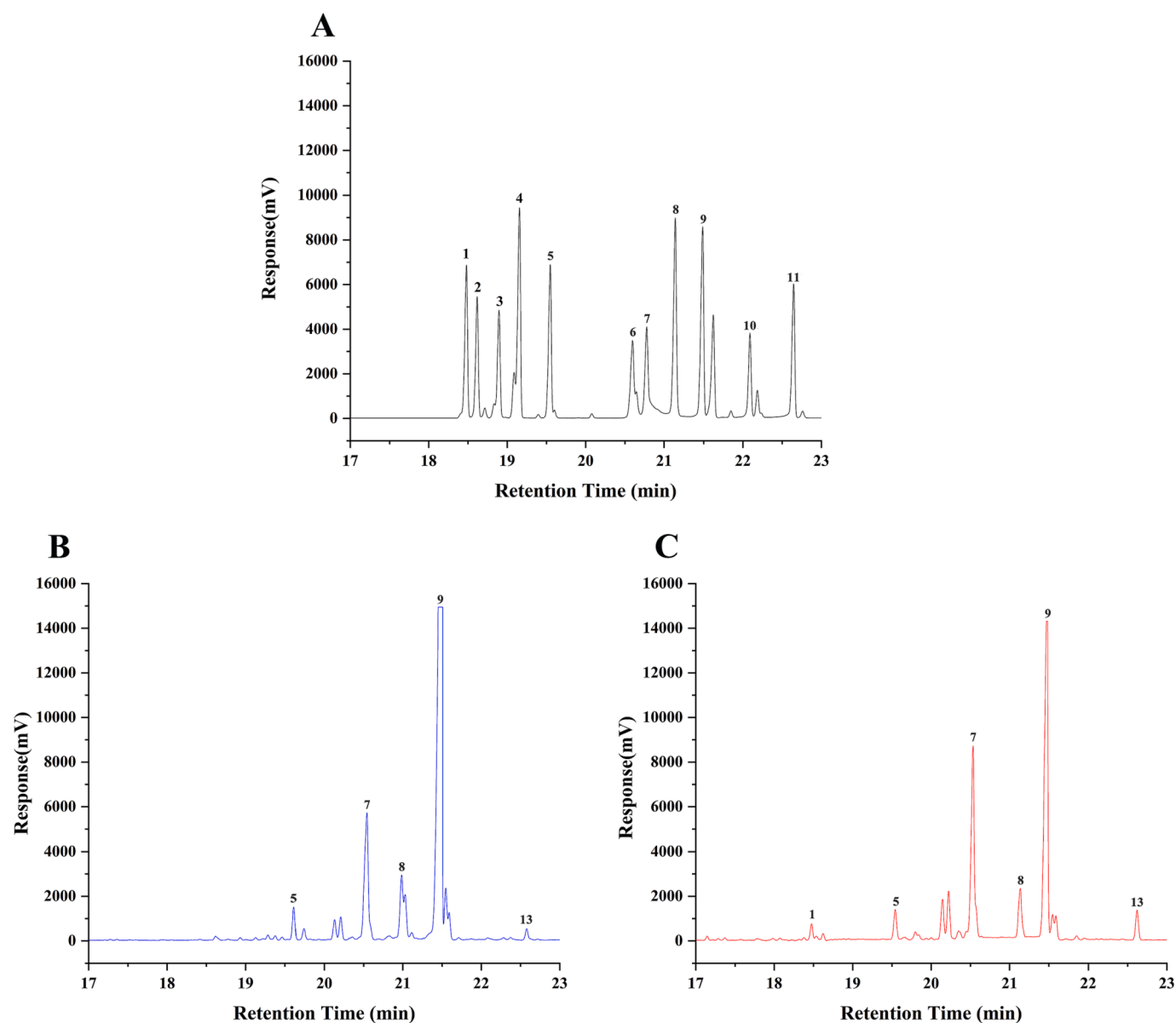


Fig. 1. Monosaccharide composition analysis of GLP and FGL. (A): GC chromatography of standard. (B): GC chromatography of GLP. (C): GC chromatography of FGLP. 1: Arabinose, 2: Rhamnose, 3: Ribose, 4: Fucose, 5: Xylose, 6: Fructose, 7: Mannose, 8: Galactose, 9: Glucose, 10: Galacturonic acid, 11: Glucuronic acid.

Table 3  
Monosaccharide composition and molecular weight of GLP and FGLP.

Samples	Mw	Monosaccharide composition (mol%)					
		Ara	Xyl	Man	Gal	Glc	GlcA
GLP	$1.12 \times 10^5$	0	1.53	15.64	1.84	80.60	0.39
FGLP	$8.89 \times 10^4$	0.42	0.82	34.31	3.32	59.47	1.66

#### Data analysis

All data were expressed in mean  $\pm$  SD, and all data were processed and statistically analyzed by Excel 2013, Origin 2018, SPSS 23.0, and GraphPad Prism (version 7.0).

## Results and discussions

### Monosaccharide composition analysis of GLP and FGLP

Monosaccharides are the most basic units of polysaccharides. The accurate determination of monosaccharide composition is crucial to elucidate the properties and structures of polysaccharides, and is beneficial to further understand the structure–activity relationship (Liu et al., 2021; Zhang et al., 2020). In this study, GC of polysaccharide samples was detected, and the monosaccharide composition of GLP and FGLP was analyzed. The results are shown in Fig. 1 and Table 3. The monosaccharide composition in this study is similar to the results of other studies, and it should be noted that the ratio of monosaccharides affects the bioactivity of polysaccharides (Liu et al., 2020; Shi et al., 2013). The mole ratio of xylose (Xyl), mannose (Man), galactose (Gal), glucose (Glc), and Glucuronic acid (GlcA) in GLP was 1.53: 15.64: 1.84: 80.6: 0.39, and the molar ratio of arabinose (Ara), Xyl, Man, Gal, Glc, and GlcA in FGLP was 0.42: 0.82: 34.31: 3.32: 59.47: 1.66. It indicated that both GLP and FGLP both were heteropolysaccharides, and their main

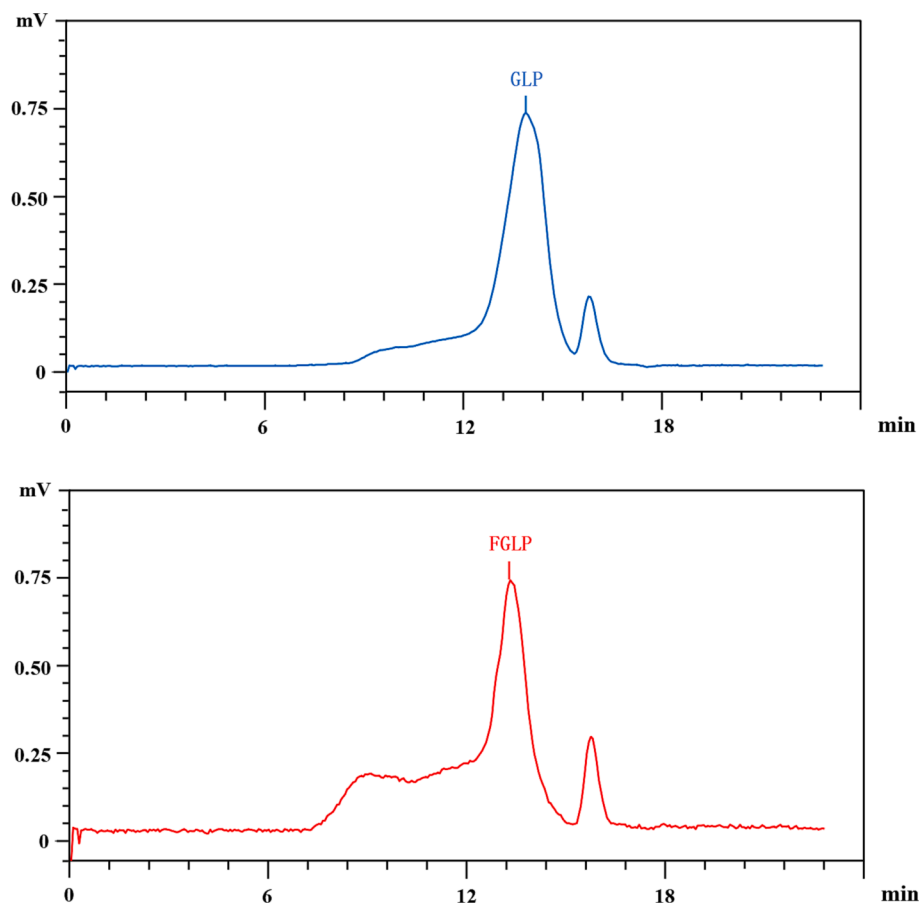


Fig. 2. High-performance gel permeation chromatogram of GLP and FGLP.

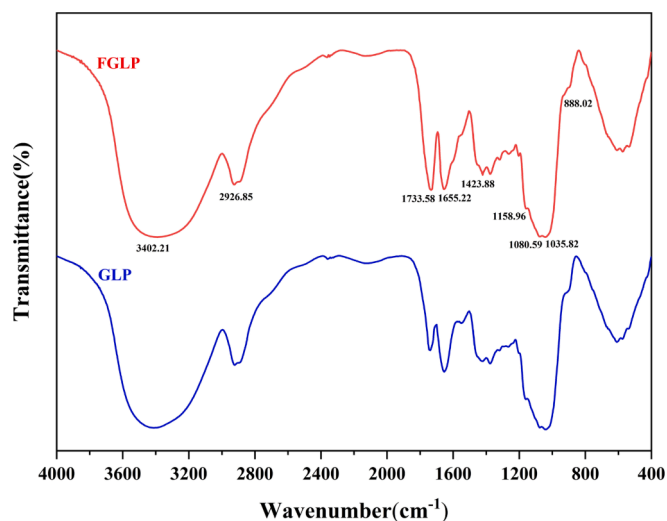


Fig. 3. FT-IR spectra of GLP and FGLP.

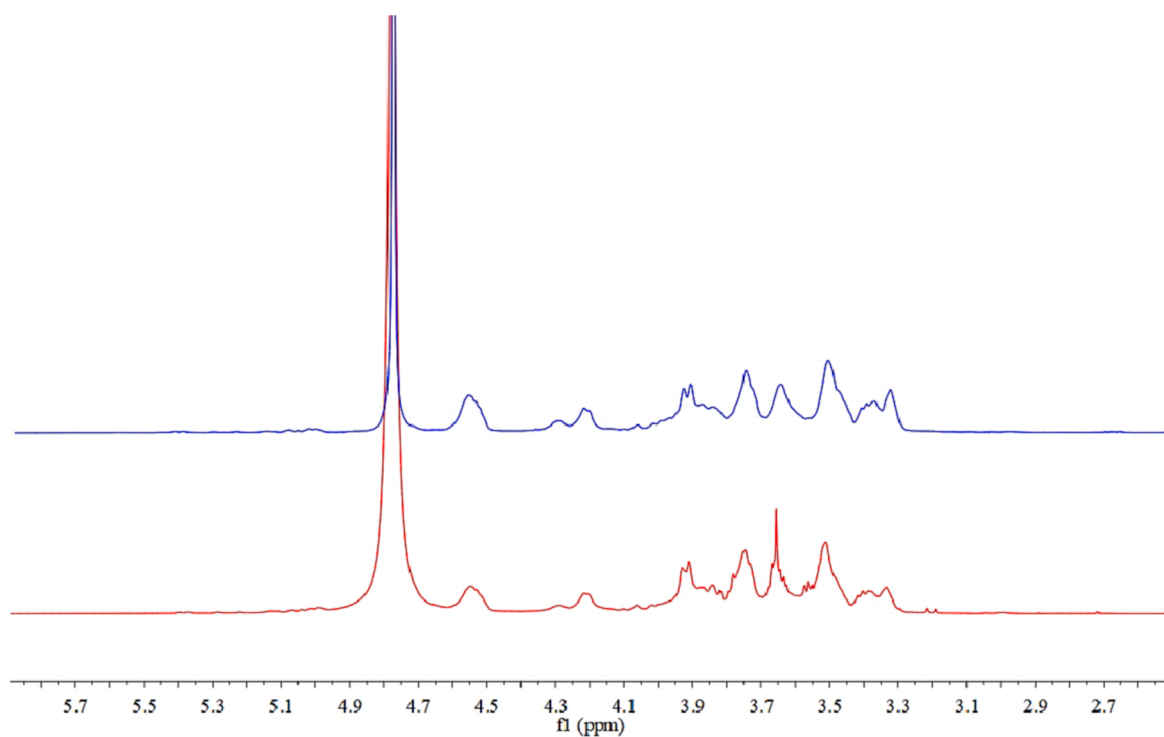
chains were composed of Glc. However, compared with GLP, the content of Man, Gal and GlcA in FGLP was increased. In contrast, the contents of Glc and Xyl were decreased, and a new monosaccharide, Ara, appeared in FGLP. In previous studies, the monosaccharide composition of *Momordica charantia* polysaccharides was significantly altered by *Lactiplantibacillus plantarum* NCU116 fermentation (Gao et al., 2018). Similarly, the monosaccharide composition of polysaccharides from *Ganoderma lucidum* spore powder in this experiment was also altered after fermentation.

#### Molecular weight analysis of GLP and FGLP

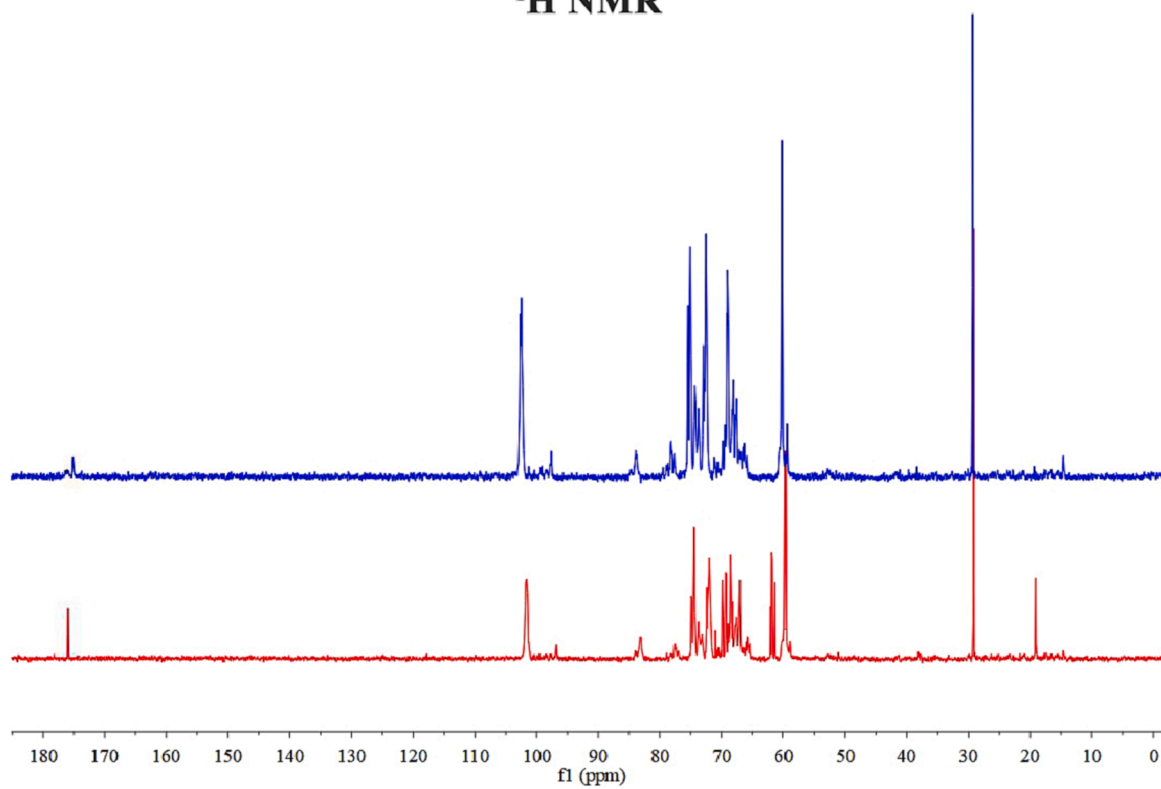
In this study, HPGPC of polysaccharide samples was detected. The results are shown in Fig. 2 and Table 3. The molecular weight of FGLP was  $8.89 \times 10^4$  Da, and that of GLP was  $1.12 \times 10^5$  Da. The antioxidant activity of *Ganoderma lucidum* polysaccharide was affected by its Molecular weight. Studies have shown that the reduction of molecular weight might increase the biological activity of polysaccharides (Kang et al., 2019). As a result, it is preliminarily speculated that fermentation could improve the antioxidant activity of *Ganoderma lucidum* polysaccharide.

#### Fourier infrared spectroscopy analysis of GLP and FGLP

The structure of polysaccharides can be determined by observing the characteristic absorption peak of the sample. As shown in Fig. 3, the absorption peaks at  $3402.21 \text{ cm}^{-1}$  of GLP and FGLP were caused by O—H stretching vibration (Wang et al., 2015). Due to C—H stretching vibration, the absorption peaks of GLP and FGLP appeared at  $2926.85 \text{ cm}^{-1}$  (Wang & Li, 2019). Due to  $\text{CH}_2$  angular vibration, the absorption peaks of GLP and FGLP appeared at  $1423.88 \text{ cm}^{-1}$  (Zeng et al., 2019). The absorption peaks at  $1400 \sim 1200 \text{ cm}^{-1}$  were caused by C—H angular vibration. The absorption peaks at  $1200 \sim 1000 \text{ cm}^{-1}$  were caused by the stretching vibration of C—O—C and C—O—H. It indicated that the characteristics of GLP and FGLP were pyranose configurations. GLP and FGLP both had absorption peaks near  $888.02 \text{ cm}^{-1}$ . It indicated that  $\beta$ -glycosidic bonds were existed in GLP and FGLP (Zheng et al., 2016). In addition, the absorption peak near  $1700 \text{ cm}^{-1}$  indicated the presence of uronic acid. The peak value of FGLP was higher than that of GLP, indicating that the content of uronic acid of polysaccharides was increased after fermentation (Rozi et al., 2019). The bioactivity of



### $^1\text{H}$ NMR



### $^{13}\text{C}$ NMR

**Fig. 4.** NMR spectrum of GLP and FGLP.  $^1\text{H}$  NMR spectrum of GLP (blue) and FGLP (red) in  $\text{D}_2\text{O}$ .  $^{13}\text{C}$  NMR spectrum of GLP (blue) and FGLP (red) in  $\text{D}_2\text{O}$ .  $^1\text{H}$ - $^{13}\text{C}$  HSQC spectrum spectra of GLP.  $^1\text{H}$ - $^{13}\text{C}$  HSQC NMR spectrum of FGLP.

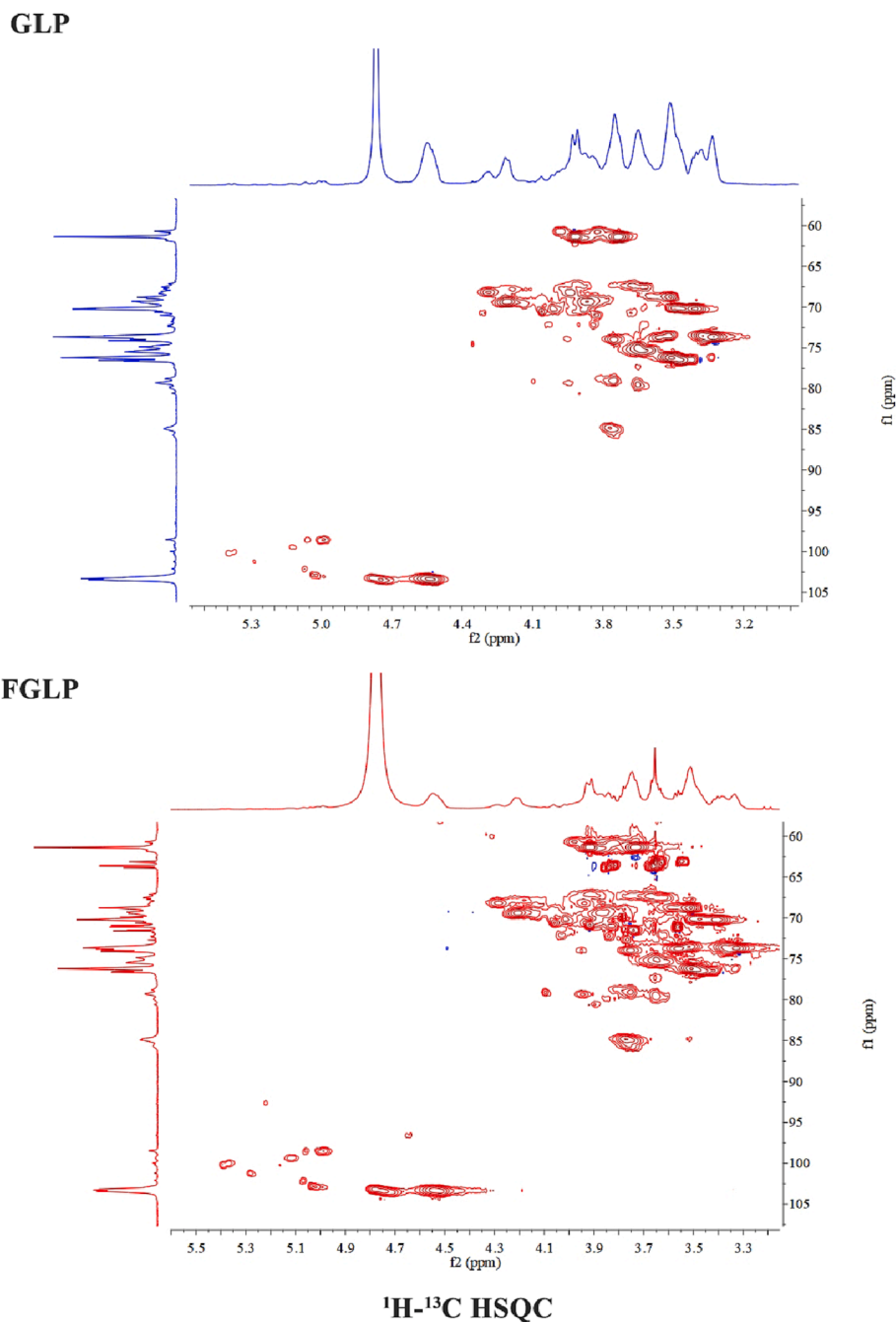


Fig. 4. (continued).

polysaccharides was proportional to the content of uronic acid, and the structures rich in uronic acid had higher antioxidant activity (Yin et al., 2021).

In conclusion, FGLP and GLP had extremely similar absorption peaks from 4000 to 400  $\text{cm}^{-1}$ , indicating that fermentation could not affect the main structure of polysaccharides in *Ganoderma lucidum* spore powder. However, the content of uronic acid in FGLP was increased, leading to improved antioxidant capacity. The above results were consistent with monosaccharide composition and NMR analysis.

#### NMR analysis

$^1\text{H}$ ,  $^{13}\text{C}$ , and HSQC spectra were scanned to identify the structural characteristics of GLP and FGLP. The spectra are shown in Fig. 4. Several anomeric signals were identified from NMR spectra in combination with

the monosaccharide composition. The chemical shift of proton peaks on the heteropolar carbon of polysaccharides within the range of 4.4–4.9 ppm corresponded to the  $\beta$  type configurations (Sheng et al., 2021). Anomeric H/C signals at 4.95/100.9 were assigned to H-1/C-1 of starch or dextrin by combining NMR data and previous literature (Sheng et al., 2021). The anomeric signals of 4.75/103.5 and 4.53/103.4 indicated  $\beta$ -1,6-Glcp and  $\beta$ -1,3-Glcp linkages were existed (Wan et al., 2021), which were located isolatedly to other anomeric signals. In the downfield of HSQC spectra, two anomeric signals were observed at 5.07/102.16 and 5.00/98.5. They were the characteristic signals of Galp (Yang et al., 2021). The signal intensity increased obviously after fermentation. It was worthy to record the intensity of 3.2–4.0 ppm in  $^1\text{H}$  spectra and 60–70 ppm in  $^{13}\text{C}$  spectra. A unique anomeric signal at 105.0 ppm was observed in  $^{13}\text{C}$  spectra, which might be assigned to  $\beta$ -Glcp and decrease dramatically after fermentation. In addition, in the

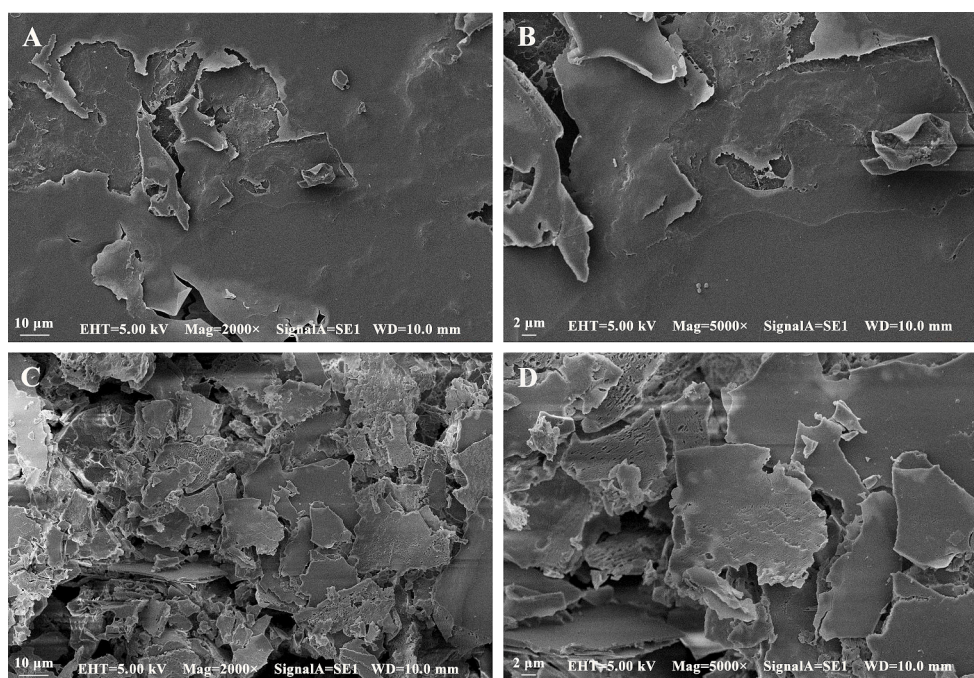


Fig. 5. Scanning electron micrographs of GLP and FGLP. (A) GLP at the magnification of  $\times 2000$ . (B) GLP at the magnification of  $\times 5000$ . (C) FGLP at the magnification of  $\times 2000$ . (D) FGLP at the magnification of  $\times 5000$ .

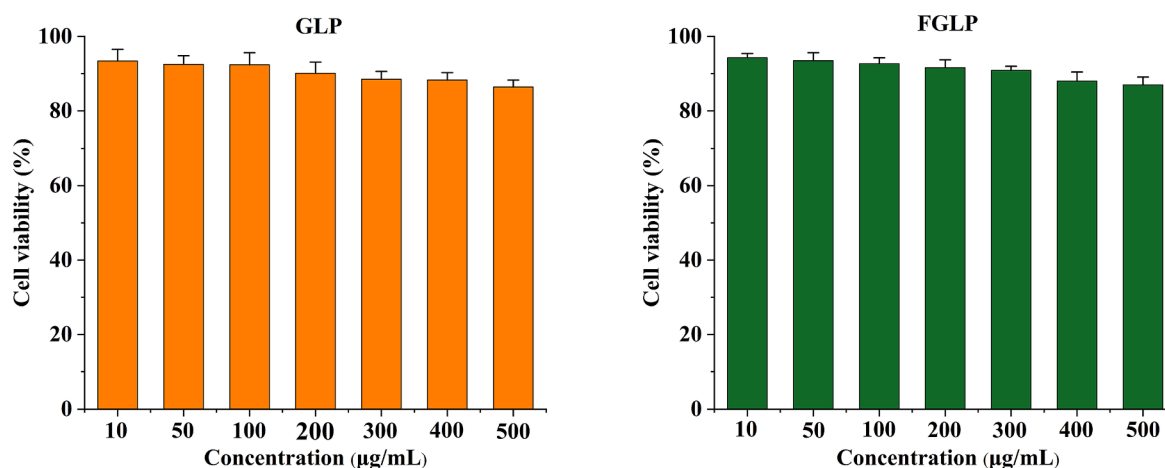


Fig. 6. Effect of different concentrations of GLP and FGLP on the viability of HepG2 cells.

$^{13}\text{C}$  spectrum, the chemical shifts at 170.0–180.0 ppm was presumed to be the signal of uronic acid, and the signal was significantly enhanced after fermentation (Zhou et al., 2021; Xu et al., 2019). In conclusion, the *Ganoderma lucidum* polysaccharides before and after fermentation were both  $\beta$ -type glucose (Sheng et al., 2021). It was found that fermentation did not affect the main structure of *Ganoderma lucidum* polysaccharides. However, the glucose content of FGLP was decreased, while the content of uronic acid was increased. The above results were the same as infrared and monosaccharide composition.

#### SEM analysis

The apparent structure of polysaccharides is very diverse, and it is difficult to observe the same apparent structure of different polysaccharides, but the changes of the apparent structure of polysaccharides before and after treatment can be well observed by electron microscopy (Cui and Zhu, 2021; Yi et al., 2011). Previous studies have shown that ultrasound can change the apparent structure of *Ganoderma*

*lucidum* polysaccharides, making its surface area significantly larger (Xu et al., 2019). In this experiment, the structure of *Ganoderma lucidum* polysaccharides also changed due to fermentation treatment. As shown in the electron microscopy (SEM) image of GLP and FGLP (Fig. 5), GLP had a smooth surface structure with loose holes, and the holes were small. The texture of GLP exhibited hard. However, FGLP had a rough surface structure with many holes, and the surface area increased significantly. From the changes of the apparent structure of polysaccharides, it can be seen that glycosidic bonds of polysaccharides in *Ganoderma lucidum* spore powder were degraded and modified to a certain extent, resulting in the changes of its apparent structure.

#### Cell culture and grouping

The cytotoxicity of GLP and FGLP was analyzed. The effect of GLP and FGLP on cells was represented by cell survival rate (Weng et al., 2009). The results are shown in Fig. 6. FGLP and GLP at concentrations of 10–500  $\mu\text{g/mL}$  were not toxic to HepG2 cells. Therefore, the

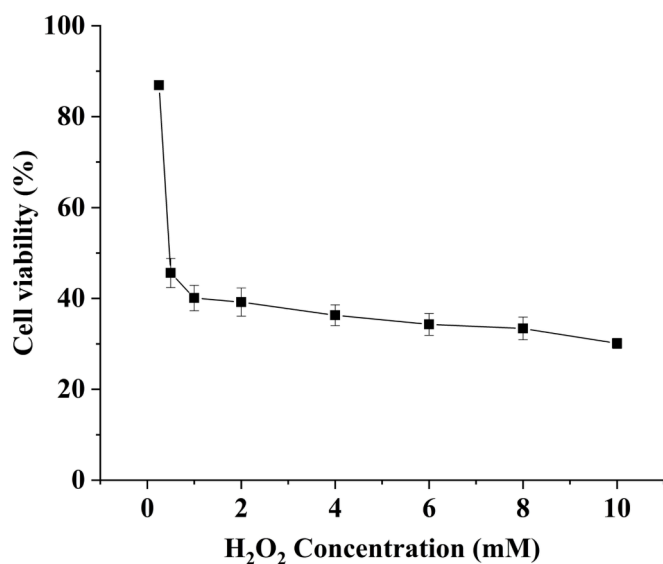


Fig. 7. Effect of different concentrations of H<sub>2</sub>O<sub>2</sub> on the viability of HepG2 cells.

concentrations of GLP and FGLP were both set as 250 µg/mL.

Hydrogen peroxide (H<sub>2</sub>O<sub>2</sub>) acts as a cell signaling molecule under normal physiological conditions. However, excessive H<sub>2</sub>O<sub>2</sub>-induced toxicity in HepG2 cells eventually leads to oxidative stress (Han et al., 2019; Zhao et al., 2021). In addition, the concentration of H<sub>2</sub>O<sub>2</sub> added to induce HepG2 was analyzed. The results are shown in Fig. 7. Within the concentration range of 0–1 mM, the cell viability of HepG2 cells was decreased sharply, and the trend got very slowly within the concentration range of 1–10 mM. It indicated that the inhibitory effect of 1 mM H<sub>2</sub>O<sub>2</sub> on HepG2 cells has reached saturation, and the survival rate was 45.6%. Therefore, the H<sub>2</sub>O<sub>2</sub> concentration was set to 1 mM.

Based on the above results, the cells were grouped as follows. Control group: The cells grew normally without additional treatment. Model group: Cells were induced by H<sub>2</sub>O<sub>2</sub> solution (1 mM). Experimental groups: After being incubated with an H<sub>2</sub>O<sub>2</sub> solution (1 mM), the cells were regulated with 250 µg/mL GLP or FGLP.

#### Effects of GLP and FGLP on intracellular ROS content in the oxidative stress model

When exogenous H<sub>2</sub>O<sub>2</sub> causes oxidative stress damage, cells produce excessive reactive oxygen species (ROS) (Li et al., 2020). DCFH-DA (2,7-dichlorofluorescein diacetate) is a classical method for detecting ROS. DCFH-DA was hydrolyzed by esterase to dichlorofluorescein (DCFH) once it entered the cell. DCFH was oxidized into dichlorofluorescein (DCF) by ROS. DCF can emit green fluorescence (Zou et al., 2018). Therefore, the accumulation of ROS in cells was exhibited by the fluorescence intensity of DCF. From Fig. 8A, the fluorescence intensity in Con was the weakest, and the fluorescence intensity in Mod was the strongest. Compared with Mod, the fluorescence intensity in the GLP group and FGLP group was weaker. It indicated that the regulatory effect of GLP and FGLP on cellular oxidative stress. For further investigation, the fluorescence intensity of each group was measured. As shown in Fig. 8B, ROS content in Mod was significantly higher than Con, indicating the oxidative stress model was successfully constructed. In contrast with the Mod group, ROS content in the GLP group and FGLP group was significantly improved. It indicated that both GLP and FGLP could significantly improve oxidative stress injury of HepG2 cells. Meanwhile, The ROS content of HepG2 cells in the GLP groups was significantly higher than that in the FGLP groups. It indicated that FGLP had a stronger ability to scavenge ROS in HepG2 cells than GLP, which preliminarily proved that the antioxidant ability of FGLP has been improved.

#### Effects of GLP and FGLP on intracellular MDA and T-AOC content in the oxidative stress model

When cells are severely damaged by oxidative stress, excessive free radicals will cause the oxidation reaction of unsaturated fatty acids on the cell membrane, and malondialdehyde (MDA) is produced. MDA will attack the cell membrane and cause damage. Therefore, MDA content can reflect the severity of cell damage caused by free radical attack (Hsieh & Wu, 2011). The level of T-AOC content can indirectly reflect the scavenging ability of cells to free radicals, which is one of the indicators to comprehensively reflect the antioxidant ability of cells (Ding and Zhao, 2018). Therefore, the antioxidant capacity of GLP and FGLP was reflected by the determination of MDA and T-AOC content in different groups. From Fig. 9, MDA content in Mod was significantly increased in contrast with Con, T-AOC content was significantly

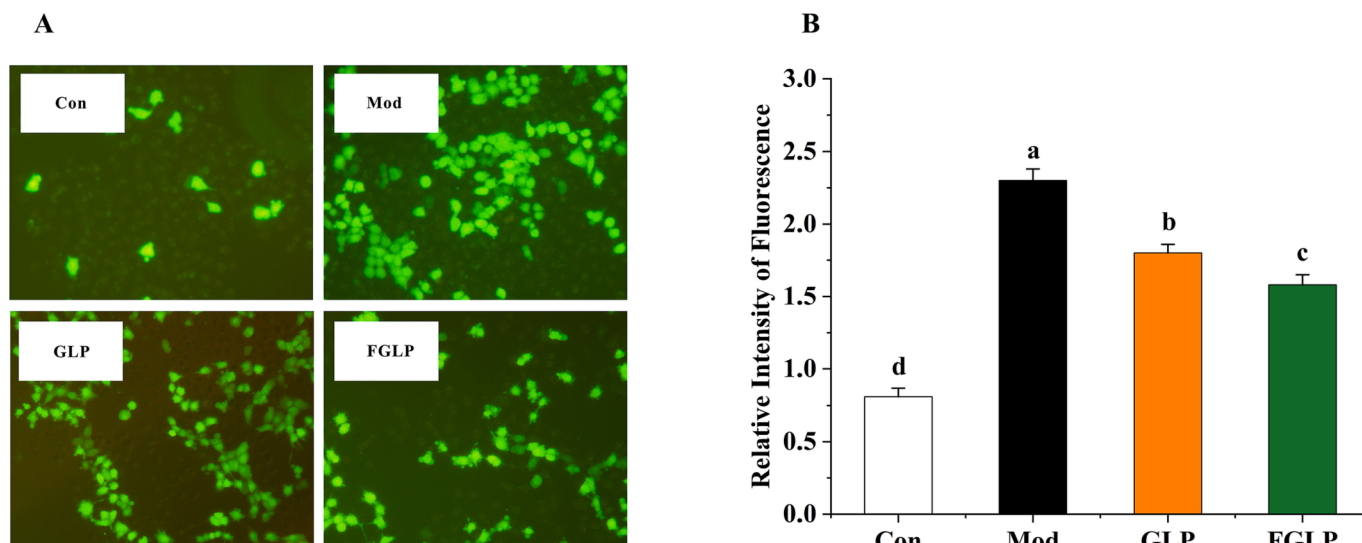


Fig. 8. The effect of GLP/FGLP on ROS activities induced by H<sub>2</sub>O<sub>2</sub> in HepG2 cells. A, The intracellular ROS in HepG2 cells after fluorescence staining was exhibited by the image; B, The relative intensity of fluorescence in different groups. Values are means ± SD (n = 3). Different letters (a–d) indicate significant differences among the different samples (p < .05, one-way ANOVA test).

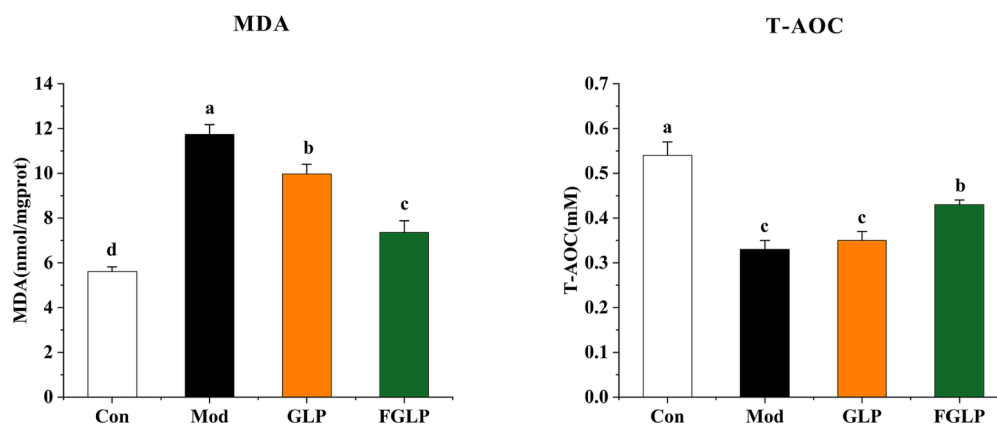


Fig. 9. Effect of GLP and FGLP on MDA and T-AOC contents in  $H_2O_2$ -induced in HepG2 cells. Values are means  $\pm$  SD ( $n = 3$ ). Different letters (a-d) indicate significant differences among the different samples ( $p < .05$ , one-way ANOVA test).

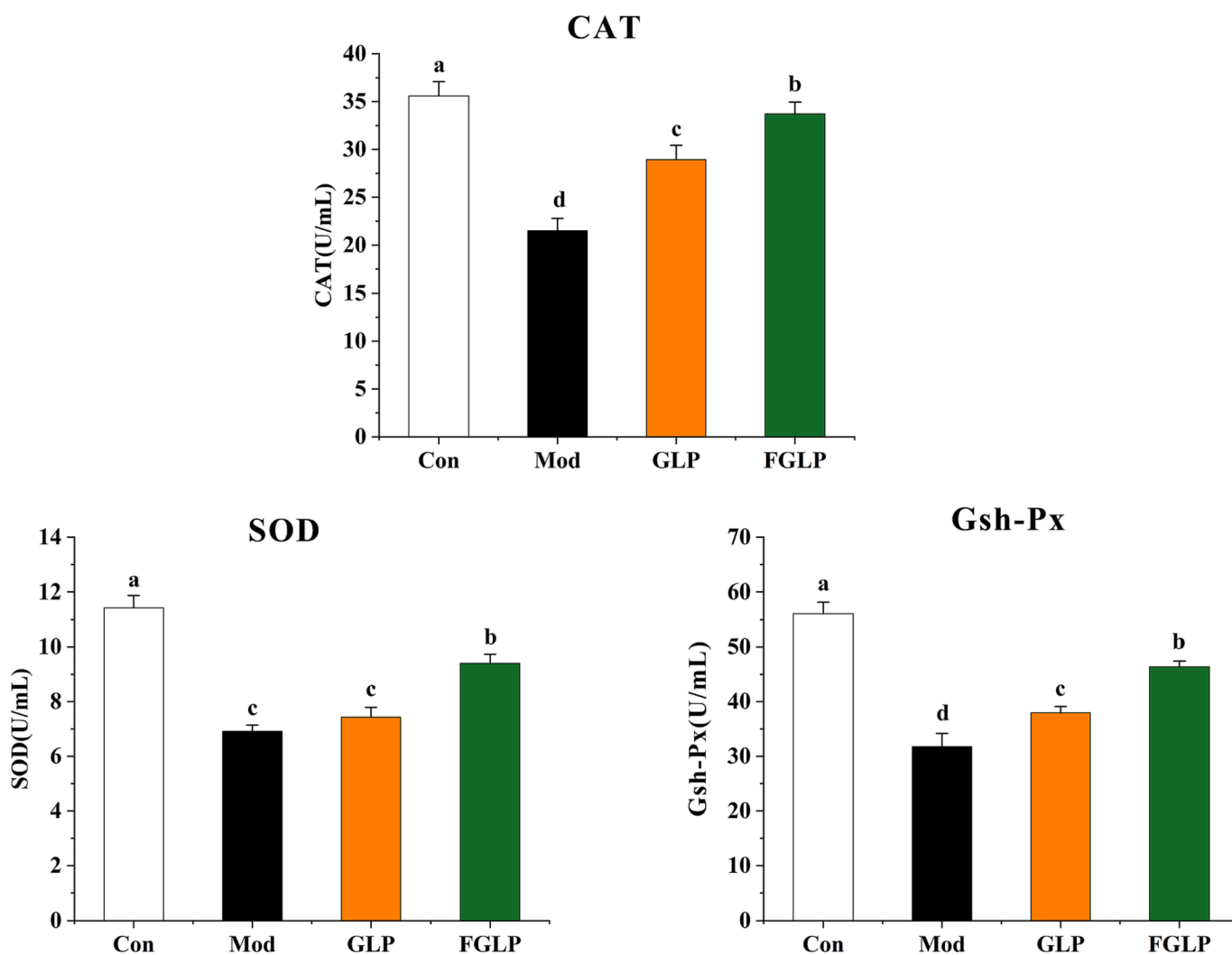
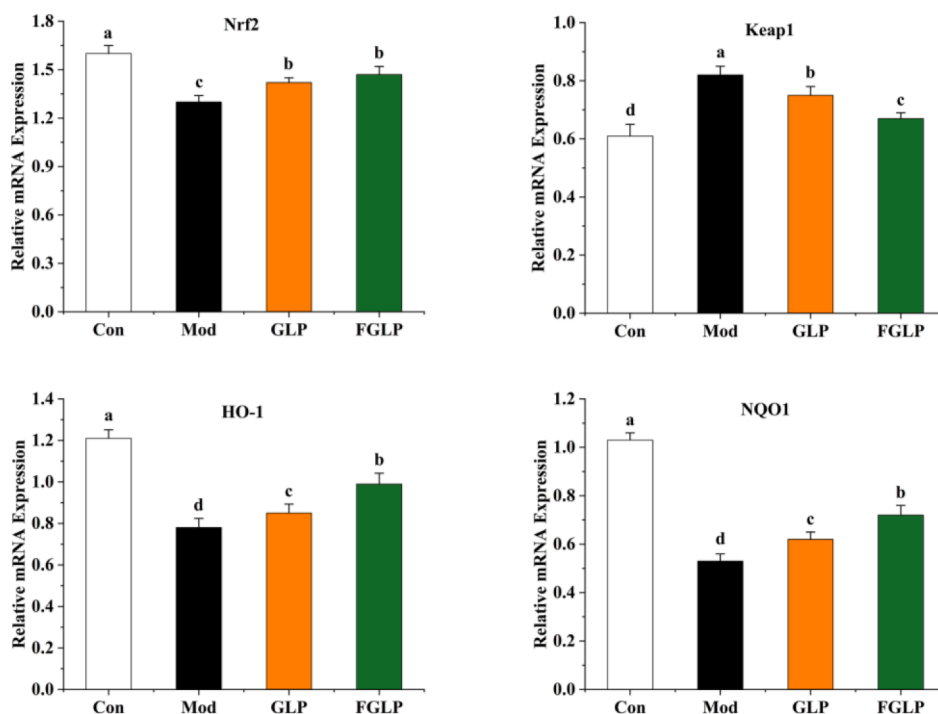


Fig. 10. Effect of GLP and FGLP on intracellular Antioxidant enzyme in  $H_2O_2$ -induced in HepG2 cells. Values are means  $\pm$  SD ( $n = 3$ ). Different letters (a-d) indicate significant differences among the different samples ( $p < .05$ , one-way ANOVA test).

decreased. It Shows that the oxidative stress model was successfully constructed. Compared with Mod, MDA contents in GLP and FGLP were significantly decreased. Meanwhile, T-AOC contents in GLP and FGLP were both increased, which was significantly in FGLP group. It indicated that both GLP and FGLP could significantly improve oxidative stress

injury of HepG2 cells. MDA content in FGLP groups was significantly higher than in the GLP groups, and T-AOC content was significantly lower. It indicated that FGLP has a more robust regulatory ability for oxidative stress model and higher antioxidant activity. The above results indicated that the antioxidant activity of *Ganoderma lucidum*



**Fig. 11.** Effect of GLP and FGLP on expression of antioxidant genes in  $H_2O_2$ -induced in HepG2 cells. Values are means  $\pm$  SD ( $n = 3$ ). Different letters (a–d) indicate significant differences among the different samples ( $p < .05$ , one-way ANOVA test).

polysaccharides was enhanced in the fermentation process.

#### *Effects of GLP and FGLP on intracellular antioxidant enzyme system in the oxidative stress model*

Under oxidative stress, the body will activate the antioxidant defense system to resist oxidative damage. The antioxidant defence system can be divided into the enzyme antioxidant system and non-enzyme antioxidant system. Among them, the enzyme antioxidant system plays an irreplaceable role in maintaining the dynamic balance of oxidative stress. SOD could catalyze the decomposition of  $O^{\cdot -2}$  into  $H_2O_2$  and  $O_2$  to scavenge free radicals. CAT could catalyze the decomposition of  $H_2O_2$  into  $H_2O$  and  $O_2$ , resulting in maintaining the dynamic redox balance of the body. GSH-Px, as a peroxide-decomposition enzyme widely existing in cells, could decompose  $H_2O_2$  into  $H_2O$  and hydroxyl compounds. Meanwhile, GSH-Px could catalyze the reaction between GSH and peroxide to remove oxides and free radicals generated in the process of cell metabolism and ultimately protect cells and the body from free radical damage. From Fig. 10, CAT, SOD, and GSH-Px contents in Mod were significantly increased in contrast with Con, indicating that the oxidative stress model was successfully constructed. CAT, SOD, and GSH-Px contents in GLP and FGLP groups were significantly decreased compared with Mod. It indicated that both GLP and FGLP could increase the content of antioxidant enzymes to improve oxidative stress injury of HepG2 cells. Previous studies have found that ganoderma lucidum polysaccharides can achieve antioxidant purposes by stimulating cell secretion of antioxidant enzymes (Sharma et al., 2019; Jia et al., 2009), and the results of this study once again confirm this view. CAT, SOD, and GSH-Px contents in the FGLP group were significantly higher than that in the GLP group. It indicated that FGLP could stimulate the body to produce more antioxidant enzymes to show more vital antioxidant ability.

#### *Effects of GLP and FGLP on expression of antioxidant genes in the oxidative stress model*

Nrf2-ARE signalling pathway is the most important oxidative stress pathway in cells. Under normal conditions, Nrf2 binds to Keap1 and remains in a static state in the cytoplasm. However, when cells are damaged by oxidative stress, Nrf2 will dissociate from Keap1 and transfer to the nucleus. It will bind to Maf protein to form dimer firstly and then bind to ARE. As a result, downstream antioxidant enzyme genes and phase II detoxification enzymes will be activated, including HO-1 and NQO1, to protect cells from oxidative stress damage (Chen et al., 2019). Previous studies have preliminarily explored the antioxidant mechanism of GLP (Li et al., 2020), and this study further verified this pathway. In this study, Keap1, Nrf2, HO-1, and NQO1 gene expression level of HepG2 cells in each group was detected to explore the mechanism of GLP and FGLP regulating oxidative stress. From Fig. 11, Nrf2 gene expression in Mod was significantly decreased in contrast with Con, while in GLP and FGLP groups were both significantly increased compared with Mod. Besides, Nrf2 gene expression in the FGLP group was higher than GLP group. Keap1 gene expression in Mod was significantly increased in contrast with Con, while in GLP and FGLP groups were both significantly decreased compared with Mod. Besides, Keap1 gene expression in the FGLP group was significantly lower than the GLP group. It indicated that FGLP and GLP could promote the dissociation of Keap1 and Nrf2 complex through down-regulation of the Keap1 gene and up-regulation of the Nrf2 gene to release more Nrf2 to resist  $H_2O_2$ -induced oxidative stress injury. Among them, FGLP has a more substantial promoting effect compared with GLP. With the transfer of Nrf2, the downstream antioxidant enzyme genes could be activated. HO-1 and NQO1 gene expressions in Mod were significantly decreased in contrast with Con, while in GLP and FGLP groups were both significantly increased compared with Mod. Besides, HO-1 and NQO1 gene expression in the FGLP group were higher than GLP group. It indicated that the antioxidant gene HO-1 and NQO1 were activated to resist  $H_2O_2$ -induced oxidative stress injury. Compared with the GLP group, the activation was more pronounced in FGLP group.

## Conclusions

In summary, *Lactiplantibacillus plantarum* ATCC14917 was used to ferment *Ganoderma lucidum* spore powder, and the changes in structure and antioxidant activity of polysaccharides after fermentation were investigated. The results showed that the main structure of polysaccharides remains unchanged. FGLP still maintained the characteristics of *Ganoderma lucidum* polysaccharide. After fermentation, the molecular weight of FGLP decreased significantly. In the monosaccharide composition, GlcA, Gal, and Man of FGLP increased significantly, while Glc and Xyl decreased significantly. The surface structure was changed from smooth and hard to porous and loose.

In terms of antioxidant activity, compared with GLP, ROS and MDA content of HepG2 cells regulated by FGLP were reduced significantly. In contrast, T-AOC content was significantly decreased, which indicated that *Lactiplantibacillus plantarum* ATCC14917 fermentation significantly improved the antioxidant activity of *Ganoderma lucidum* polysaccharides. In terms of the regulatory mechanism, the Nrf2-ARE pathway in cells was regulated by GLP and FGLP to release antioxidant enzymes CAT, SOD, and Gsh-Ps. Compared with the GLP group, the activation was more pronounced in FGLP group.

The biological activity of polysaccharides is closely associated with their structure. The increased antioxidant activity of FGLP may be caused by the increased uronic acid and the decreased molecular weight. Nonetheless, the mechanism of the increased antioxidant activity of FGLP still needs to be further investigated.

## CRedit authorship contribution statement

**Yang Zhao:** Conceptualization, Methodology, Formal analysis, Writing – original draft. **Qinyang Li:** Software, Formal analysis. **Minghui Wang:** Investigation. **Yuhua Wang:** . **Chunhong Piao:** Investigation. **Hansong Yu:** . **Junmei Liu:** Funding acquisition, Writing – review & editing, Supervision. **Zhuowei Li:** Funding acquisition, Writing – review & editing, Supervision.

## Declaration of Competing Interest

The authors declare that they have no known competing financial interests or personal relationships that could have appeared to influence the work reported in this paper.

## Data availability

The data that has been used is confidential.

## Acknowledgements

This study was supported by the Program of Science and Technology Development Plan of Jilin Province (No. 20200301026RQ).

## References

- Chen, L., Li, K., Liu, Q., Quiles, J. L., Filosa, R., Kamal, M. A., & Xiao, J. (2019). Protective effects of raspberry on the oxidative damage in HepG2 cells through Keap1/Nrf2-dependent signaling pathway. *Food and Chemical Toxicology*, *133*, Article 110781.
- Chiroma, A. A., Khaza'ai, H., Abd. Hamid, R., Chang, S. K., Zakaria, Z. A., Zainal, Z. (2020). Analysis of expression of vitamin E-binding proteins in H<sub>2</sub>O<sub>2</sub> induced SK-N-SH neuronal cells supplemented with  $\alpha$ -tocopherol and tocotrienol-rich fraction. *Plos One*, *15*, e0241112.
- Čor, D., Knez, Ž., & Knez Hrncić, M. (2018). Antitumour, antimicrobial, antioxidant and antiacetylcholinesterase effect of ganoderma lucidum terpenoids and polysaccharides: A review. *Molecules*, *23*, 649.
- Cui, R., & Zhu, F. (2021). Ultrasound modified polysaccharides: A review of structure, physicochemical properties, biological activities and food applications. *Trends in Food Science & Technology*, *107*, 491–508.
- Ding, H., & Zhao, B. (2018). Change characteristics of women boxers' Na<sup>+</sup>, K<sup>+</sup>-ATPase, ROS and T-AOC before the match. *Energy Procedia*, *17*, 671–677.

- Gao, H., Wen, J. J., Hu, J. L., Nie, Q. X., Chen, H. H., Xiong, T., ... Xie, M. Y. (2018). Polysaccharide from fermented *Momordica charantia* L. with *Lactobacillus plantarum* NCU116 ameliorates type 2 diabetes in rats. *Carbohydrate polymers*, *201*, 624–633.
- Garuba, T., Olahan, G. S., Lateef, A. A., Alaya, R. O., Awolowo, M., & Sulyman, A. (2020). Proximate composition and chemical profiles of reishi mushroom (*Ganoderma lucidum* (Curt: Fr.) Karst). *Arab Gulf Journal of Scientific Research*, *12*, 103–110.
- Han, J. M., Lee, E. K., Gong, S. Y., Sohng, J. K., Kang, Y. J., & Jung, H. J. (2019). *Sparassis crispa* exerts anti-inflammatory activity via suppression of TLR-mediated NF- $\kappa$ B and MAPK signaling pathways in LPS-induced RAW264. 7 macrophage cells. *Journal of Ethnopharmacology*, *231*, 10–18.
- Hao, G. P. (2018). Study and analysis of human hepatocellular carcinoma cell named HepG2 culture method. *Journal of University of Science and Technology of China*, *20*, 7–10.
- Hsieh, T. C., & Wu, J. M. (2011). Suppression of proliferation and oxidative stress by extracts of *Ganoderma lucidum* in the ovarian cancer cell line OVCAR-3. *The International Journal of Medicinal Mushrooms*, *28*(6), 1065–1069.
- Jia, J., Zhang, X., Hu, Y. S., Wu, Y., Wang, Q. Z., Li, N. N., ... Dong, X. C. (2009). Evaluation of in vivo antioxidant activities of *Ganoderma lucidum* polysaccharides in STZ-diabetic rats. *Food Chemistry*, *115*(1), 32–36.
- Kang, Q., Chen, S., Li, S., Wang, B., Liu, X., Hao, L., & Lu, J. (2019). Comparison on characterization and antioxidant activity of polysaccharides from *Ganoderma lucidum* by ultrasound and conventional extraction. *International Journal of Biological Macromolecules*, *124*, 1137–1144.
- Kan, Y., Chen, T., Wu, Y., & Wu, J. (2015). Antioxidant activity of polysaccharide extracted from *Ganoderma lucidum* using response surface methodology. *International Journal of Biological Macromolecules*, *72*, 151–157.
- Li, H. N., Zhao, L. L., & Di Yi Zhou, D. Q. C. (2020). *Ganoderma lucidum* polysaccharides ameliorates hepatic steatosis and oxidative stress in db/db mice via targeting nuclear factor E2 (Erythroid-Derived 2)-related factor-2/heme oxygenase-1 (HO-1) pathway. *Medical Science Monitor*, *26*, e921905-1.
- Li, J., Gu, F., Cai, C., Hu, M., Fan, L., Hao, J., & Yu, G. (2020). Purification, structural characterization, and immunomodulatory activity of the polysaccharides from *Ganoderma lucidum*. *International Journal of Biological Macromolecules*, *143*, 806–813.
- Li, S., Hao, L., Kang, Q., Cui, Y., Jiang, H., Liu, X., & Lu, J. (2017). Purification, characterization and biological activities of a polysaccharide from *Lepidium meyenii* leaves. *International Journal of Biological Macromolecules*, *103*, 1302–1310.
- Li, S., Hao, L., Kang, Q., Cui, Y., Jiang, H., Liu, X., & Lu, J. (2018). Structural characteristics and bioactive properties of a novel polysaccharide from *Flammulina velutipes*. *Carbohydrate Polymers*, *197*, 147–156.
- Liu, J., He, R., Sun, P., Zhang, F., Linhardt, R. J., & Zhang, A. (2020). Molecular mechanisms of bioactive polysaccharides from *Ganoderma lucidum* (Lingzhi), a review. *International Journal of Biological Macromolecules*, *150*, 765–774.
- Liu, Y., Wang, Y., Zhou, S., Yan, M., Tang, Q., & Zhang, J. (2021). Structure and chain conformation of bioactive  $\beta$ -D-glucan purified from water extracts of *Ganoderma lucidum* unbroken spores. *International Journal of Biological Macromolecules*, *180*, 484–493.
- Livak, K. J., & Schmittgen, T. D. (2001). Analysis of relative gene expression data using real-time quantitative PCR and the 2(-Delta Delta C(T)) method. *Methods*, *25*(4), 402–408.
- Li, Y. Q., Fang, L., & Zhang, K. C. (2007). Structure and bioactivities of a galactose rich extracellular polysaccharide from submergedly cultured *Ganoderma lucidum*. *Carbohydrate Polymers*, *68*, 323–328.
- Li, Z., Teng, J., Lyu, Y., Hu, X., Zhao, Y., & Wang, M. (2018). Enhanced antioxidant activity for apple juice fermented with *Lactobacillus Plantarum* ATCC14917. *Molecules*, *24*, 51.
- Nie, Q., Hu, J., Gao, H., Fan, L., Chen, H., & Nie, S. (2019). Polysaccharide from *Plantago asiatica* L. attenuates hyperglycemia, hyperlipidemia and affects colon microbiota in type 2 diabetic rats. *Food Hydrocolloids*, *86*, 34–42.
- Pan, K., Jiang, Q., Liu, G., Miao, X., & Zhong, D. (2013). Optimization extraction of *Ganoderma lucidum* polysaccharides and its immunity and antioxidant activities. *International Journal of Biological Macromolecules*, *55*, 301–306.
- Rozi, P., Abuduwaili, A., Mutailifu, P., Gao, Y., Rakhmanberdieva, R., Aisa, H. A., & Yili, A. (2019). Sequential extraction, characterization and antioxidant activity of polysaccharides from *Fritillaria pallidiflora* Schrenk. *International Journal of Biological Macromolecules*, *131*, 97–106.
- Sharma, C., Bhardwaj, N., Sharma, A., Tuli, H. S., Batra, P., Beniwal, V., ... Sharma, A. K. (2019). Bioactive metabolites of *Ganoderma lucidum*: Factors, mechanism and broad spectrum therapeutic potential. *Journal of Herbal Medicine*, *17*, Article 100268.
- Sheng, Z., Liu, J., & Yang, B. (2021). Structure differences of water soluble polysaccharides in *Astragalus membranaceus* induced by origin and their bioactivity. *Foods*, *10*(8), 1755.
- Sheng, Z., Wen, L., & Yang, B. (2021). Structure identification of a polysaccharide in mushroom *Lingzhi* spore and its immunomodulatory activity. *Carbohydrate Polymers*, *278*, Article 118939.
- Shi, M., Zhang, Z., & Yang, Y. (2013). Antioxidant and immunoregulatory activity of *Ganoderma lucidum* polysaccharide (GLP). *Carbohydrate Polymers*, *95*, 200–206.
- Sun, H., Ni, X., Song, X., Wen, B., Zhou, Y., Zou, F., & Wang, P. (2016). Fermented *Yupingfeng* polysaccharides enhance immunity by improving the foregut microflora and intestinal barrier in weaning rex rabbits. *Applied Microbiology and Biotechnology*, *100*, 8105–8120.
- Tan, X., Sun, J., Xu, Z., Li, H., Hu, J., Ning, H., & Zhang, X. (2018). Effect of heat stress on production and in-vitro antioxidant activity of polysaccharides in *Ganoderma lucidum*. *Bioprocess and Biosystems Engineering*, *41*, 135–141.
- Tian, W., Dai, L., Lu, S., Luo, Z., Qiu, Z., Li, J., Du, B. Effect of *Bacillus* sp. (2019). DU-106 fermentation on *Dendrobium officinale* polysaccharide: Structure and

- immunoregulatory activities. *International Journal of Biological Macromolecules*, *135*, 1034–1042.
- Veljović, S., Veljović, M., Nikićević, N., Despotović, S., Radulović, S., Nikšić, M., & Filipović, L. (2017). Chemical composition, antiproliferative and antioxidant activity of differently processed *Ganoderma lucidum* ethanol extracts. *Journal of Food Science and Technology-Ukraine*, *54*, 1312–1320.
- Wang, F., Wang, W., Huang, Y., Liu, Z., & Zhang, J. (2015). Characterization of a novel polysaccharide purified from a herb of *Cynomorium songaricum* Rupr. *Food Hydrocolloids*, *47*, 79–86.
- Wang, H., Liu, Y. M., Qi, Z. M., Wang, S. Y., Liu, S. X., Li, X., & Xia, X. C. (2013). An overview on natural polysaccharides with antioxidant properties. *Medicinal Chemistry*, *20*, 2899–2913.
- Wang, L., & Li, X. (2019). Preparation, physicochemical property and in vitro antioxidant activity of zinc-Hohenbuehelia serotina polysaccharides complex. *International Journal of Biological Macromolecules*, *121*, 862–869.
- Wan, Y. J., Hong, T., Shi, H. F., Yin, J. Y., Koev, T., Nie, S. P., & Xie, M. Y. (2021). Probiotic fermentation modifies the structures of pectic polysaccharides from carrot pulp. *Carbohydrate Polymers*, *251*, Article 117116.
- Weng, C. J., Chau, C. F., Yen, G. C., Liao, J. W., Chen, D. H., & Chen, K. D. (2009). Inhibitory effects of *Ganoderma lucidum* on tumorigenesis and metastasis of human hepatoma cells in cells and animal models. *Journal of Agricultural and Food Chemistry*, *57*(11), 5049–5057.
- Xu, Y., Zhang, X., Yan, X. H., Zhang, J. L., Wang, L. Y., Xue, H., & Liu, X. J. (2019). Characterization, hypolipidemic and antioxidant activities of degraded polysaccharides from *Ganoderma lucidum*. *International Journal of Biological Macromolecules*, *135*, 706–716.
- Yang, Y., Chang, Y., Wu, Y., Liu, H., Liu, Q., Kang, Z., & Duan, J. (2021). A homogeneous polysaccharide from *Lycium barbarum*: Structural characterizations, anti-obesity effects and impacts on gut microbiota. *International Journal of Biological Macromolecules*, *183*, 2074–2087.
- Yin, D., Sun, X., Li, N., Guo, Y., Tian, Y., & Wang, L. (2021). Structural properties and antioxidant activity of polysaccharides extracted from *Laminaria japonica* using various methods. *Process Biochemistry*, *111*, 201–209.
- Yi, W. S., Qin, L. H., & Cao, J. B. (2011). Investigation of morphological change of green tea polysaccharides by SEM and AFM. *Scanning*, *33*(6), 450–454.
- Zeng, X., Li, P., Chen, X., Kang, Y., Xie, Y., Li, X., & Zhang, Y. (2019). Effects of deproteinization methods on primary structure and antioxidant activity of *Ganoderma lucidum* polysaccharides. *International Journal of Biological Macromolecules*, *126*, 867–876.
- Zhang, M., Zhang, Y., Ma, X., Liu, X., Niu, M., Yao, R., & Zhang, L. (2020). Using a PCR instrument to hydrolyze polysaccharides for monosaccharide composition analyses. *Carbohydrate polymers*, *240*, Article 116338.
- Zhang, Z. H., Fan, S. T., Huang, D. F., Yu, Q., Liu, X. Z., Li, C., & Xie, M. Y. (2018). Effect of *Lactobacillus Plantarum* NCU116 fermentation on *Asparagus officinalis* polysaccharide: Characterization, Antioxidative, and Immunoregulatory activities. *Journal of Agricultural and Food Chemistry*, *66*, 10703–10711.
- Zhao, L., Dong, Y., Chen, G., & Hu, Q. (2010). Extraction, purification, characterization and antitumor activity of polysaccharides from *Ganoderma lucidum*. *Carbohydrate Polymers*, *80*, 783–789.
- Zhao, Y., Liu, S., Sheng, Z., Li, X., Chang, Y., Dai, W., ... Yang, Y. (2021). Effect of pinolenic acid on oxidative stress injury in HepG2 cells induced by H<sub>2</sub>O<sub>2</sub>. *Food Science & Nutrition*, *9*(10), 5689–5697.
- Zheng, Y., Zhang, S., Wang, Q., Lu, X., Lin, L., Tian, Y., & Zheng, B. (2016). Characterization and hypoglycemic activity of a β-pyran polysaccharides from bamboo shoot (*Leleba oldhami* Nakai) shells. *Carbohydrate Polymers*, *144*, 438–446.
- Zhou, S., Huang, G., & Chen, G. (2021). Extraction, structural analysis, derivatization and antioxidant activity of polysaccharide from Chinese yam. *Food Chemistry*, *361*, Article 130089.
- Zhu, K., Zhang, Y., Nie, S., Xu, F., He, S., Gong, D., & Tan, L. (2017). Physicochemical properties and in vitro antioxidant activities of polysaccharide from *Artocarpus heterophyllus* Lam. Pulp. *Carbohydrate Polymers*, *155*, 354–361.
- Zou, B., Xiao, G., Xu, Y., Wu, J., Yu, Y., & Fu, M. (2018). Persimmon vinegar polyphenols protect against hydrogen peroxide-induced cellular oxidative stress via Nrf2 signalling pathway. *Food Chemistry*, *255*, 23–30.